Materials Science-Poland, Vol. 26, No. 3, 2008

Dielectric and structural characteristics of Sm doped $Ba_4La_{9.33}Ti_{18}O_{54}$ ceramics

S. BAHEL, S. BINDRA NARANG[*]

Department of Electronics Technology, Guru Nanak Dev University, Amritsar, Punjab, India

The microwave dielectric properties and structural variation of Sm doped $Ba_4La_{9.33}Ti_{18}O_{54}$ have been investigated. $Ba_4(La_{1-y}Sm_y)_{9.33}Ti_{18}O_{54}$, $y = 0.0$–0.7 ceramics were prepared by conventional solid state route. The electric permittivity and loss tangent were measured using a network analyzer in the frequency range of 0.3–3.0 GHz at room temperature. The loss tangent decreases significantly upon increasing Sm contents, along with a slight reduction in electric permittivity. A relatively good combination of dielectric properties was obtained for $y = 0.5$ ($\varepsilon' = 83.3$ and $\tan\delta = 0.021$ at 3.0 GHz). X-ray diffraction and scanning electron microscopy were applied to investigate the microstructure and correlate it with microwave dielectric properties.

Key words: *ceramics; X-ray diffraction; scanning electron microscopy; electric permittivity; loss tangent*

1. Introduction

The latest development in mobile communication increased the need for good quality microwave dielectric ceramics to be used as resonators, band pass filters and duplexers. The ceramics required for these devices should have a high electric permittivity (ε') and a low dielectric loss (or loss tangent) or high quality factor ($Q = 1/\tan\delta$). The ceramics based on a BaO–R_2O_3–TiO_2 (R = rare earth; Sm, Nd, Pr, La) ternary system has been extensively investigated [1–3]. In this system, $Ba_{6-3x}R_{8+2x}Ti_{18}O_{54}$ solid solutions showing high electric permittivity were discovered on the tie line joining $BaTiO_3$ and R_2TiO_5 composition [4]. The $Ba_{6-3x}R_{8+2x}Ti_{18}O_{54}$ solid solution shows a tungsten bronze-type structure with orthorhombic symmetry. The fundamental structural formula of this compound was reported [5] as $[R_{8+2x}Ba_{2-3x}V_x]_{A1}[Ba_4]_{A2}[V_4]_C Ti_{18}O_{54}$, where V is vacancy, A1-site is rhombic forming 2×2 perovskite block, while A2-site and *C*-site are pentagonal and trigonal ones, respectively. Three different cations with different diameters occupy different sites – the middle sized R ions

---

[*] Corresponding author, e-mail: sukhleen2@yahoo.com

mainly occupy A1-sites; the largest Ba ions occupy A2-sites and A1 sites and the smallest Ti ions alone occupy octahedral *B* sites. At $x = 2/3$, the R and Ba cations separately occupy A1 and A2 sites which leads to the highest *Q* value or the lowest loss tangent [5, 6]. Under special conditions of R = La and $x = 2/3$, the composition $Ba_4La_{9.33}Ti_{18}O_{54}$ exhibits the highest electric permittivity with the highest dielectric loss [5, 7].

The purpose of this paper is to reduce the loss without much change in electric permittivity. The Sm substitution in place of Nd has been shown [8–10] effective in reducing the loss of barium neodymium titanate (similar material). It attracted the attention and provided the motivation to study the effect of Sm doping on microwave dielectric properties of $Ba_4La_{9.33}Ti_{18}O_{54}$.

2. Experimental

Samples of $Ba_4(La_{1-y}Sm_y)_{9.33}Ti_{18}O_{54}$ with y = 0.0, 0.1, 0.3, 0.5 and 0.7 were synthesized by conventional solid state method from individual reagent grade oxide powders – BaO (99.5%), La_2O_3 (99.9%), Sm_2O_3 (99.9%) and TiO_2 (99.5%). Stoichiometric proportions of the raw materials were mixed in agate mortar for 12 h in methanol, dried and calcined at 1100 °C for 2 h. The calcined powders were ground again for 12 h and an organic binder, 3 wt. % PVA (poly (vinyl alcohol)), was added. These were then passed through a mesh and pressed to pellets of various shapes under the load of 98 kN. These pellets were then sintered at 1300 °C for 2h in air in a linearly programmable furnace. The sintered pellets were polished with fine emery paper to make the surfaces flat, smooth and parallel for measurements.

These samples were then characterized for various properties. X-ray powder diffraction (XRD) patterns were recorded with powders of sintered samples using Ni filtered CuK_α radiation in the 20–80° 2θ range (model PWQ 1729, Philips). From these patterns, lattice parameters were calculated by the least square method. The internal strain/fluctuation of *d*-spacing η was obtained from the following equation [5] as the grain size of the ceramics is sufficiently large:

$$\eta = \frac{\beta}{2\tan\theta} \tag{1}$$

where β is the full-width at half-maximum (FWHM) and is calculated using a computer program.

The bulk densities were measured by the liquid displacement method (Archimedes method) [11]. The micro-structural observation was carried out by scanning electron microscopy (model JSM 6100, JEOL Japan). The electric permittivity and loss tangent were measured by coaxial open ended probe method [12] using network analyzer (model 8714ET, Agilent Technologies) in the frequency range 0.3–3.0 GHz at room temperature.

3. Results and discussion

Figure 1 shows the XRD patterns of $Ba_4(La_{1-y}Sm_y)_{9.33}Ti_{18}O_{54}$ ceramics with various Sm contents. The patterns are identified with tungsten bronze-type compounds and match with the one reported for $Ba_4La_8Ti_{17}O_{50}$ (JCPDS file no 42-0419). All the peaks are indexed and there is no evidence of any secondary phase present for $y < 0.5$. However for $y = 0.7$, all peaks are assigned to tungsten bronze-type $BaSm_2Ti_4O_{12}$ structure (JCPDS file no 44-62). A small amount of a secondary phase, identified as $Ba_4La_8Ti_{17}O_{50}$, is also detected. All the solid solutions have the perovskite structure with an orthorhombic symmetry.

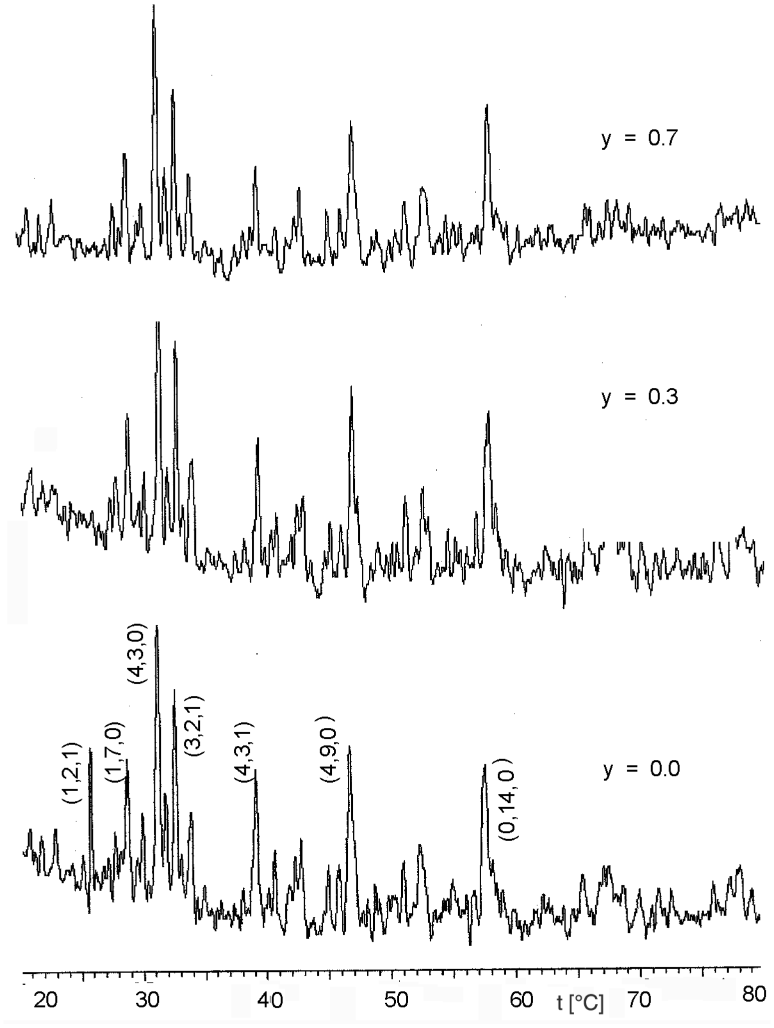

Fig. 1. X ray diffraction patterns for $Ba_4(La_{(1-y)}Sm_y)_{9.33}Ti_{18}\,O_{54}$

The lattice parameters for different Sm contents are given in Table 1. The variation of unit cell volume with increasing Sm contents is shown in Fig. 2.

Table 1. Variation of lattice parameters for different Sm contents

Composition y	a [Å]	b [Å]	c [Å]
0.0	12.33	22.41	3.87
0.1	12.32	22.38	3.85
0.3	12.31	22.35	3.85
0.5	12.26	22.18	3.81
0.7	12.19	22.12	3.78

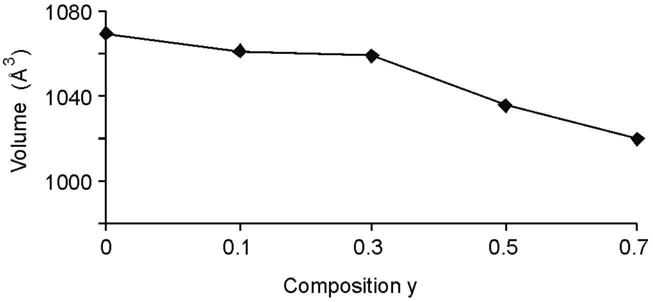

Fig. 2. Cell volumes for various Sm contents

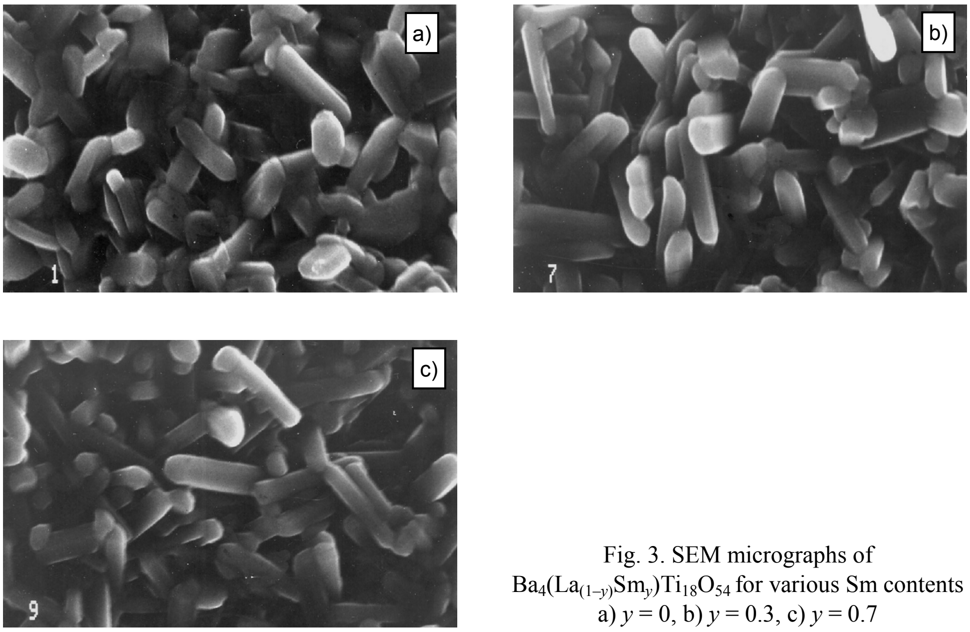

Fig. 3. SEM micrographs of $Ba_4(La_{(1-y)}Sm_y)Ti_{18}O_{54}$ for various Sm contents a) $y = 0$, b) $y = 0.3$, c) $y = 0.7$

The lattice parameters gradually decrease as the amount of Sm substitution for La increases with maximum change for *c*-axis and minimum for *a*-axis. However, with respect to changes per Å, the maximum change is 2.32% for *c*-axis, the minimum is 1.13% for *a*-axis and the change for *b*-axis is 1.29%. The change in lattice parameters could be attributed to the change in ionic radius between La and Sm ions. Shannon [13] reported the effective ionic radii for 12 co-ordinations as 1.36 Å and 1.24 Å for La and Sm ions, respectively. The difference of ionic radii directly affects the lattice parameters because a repetition of the rhombic and pentagonal sites stacked along *c*-axis brings out the length of lattice parameters.

The SEM micrographs of fractured surface of the sintered samples are shown in Fig. 3. The ceramics have a close microstructure with low porosity and closely packed hexagonal grain. It shows that the average grain size decreases slightly with increase in Sm contents.

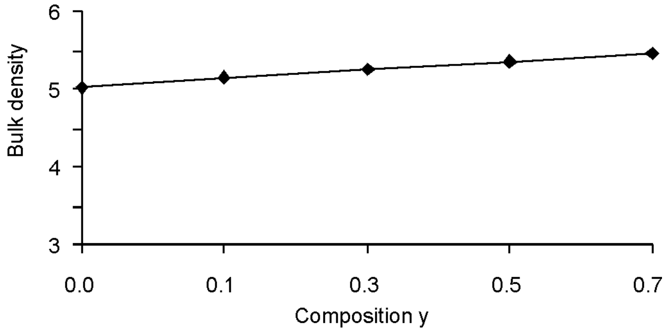

Fig. 4. Bulk densities (in g/cm^3) for various Sm contents

The bulk densities of $Ba_4(La_{1-y}Sm_y)_{9.33}Ti_{18}O_{54}$ ceramics as a function of increasing Sm contents are shown in Fig. 4. The ceramics have a high value of bulk density (> 5.0 g/cm^3) with a maximum of 5.45 g/ cm^3 for $y = 0.7$.

The electric permittivities and loss tangents of all the ceramics are shown in Figs. 5 and 6, respectively, in functions of frequency in 0.3–3.0 GHz region at room temperature. The electric permittivity decreases from 93.04 to 81.02 and loss tangent also decreases from 0.1659 to 0.012 at 3.0 GHz with increase in Sm contents. The dielectric properties of the solid solutions are highly influenced by the crystal structure. Table 1 shows that the lattice parameters decrease with increase in Sm substitution for La. This decrease in lattice parameters may lead to shrinkage of *B*-sites occupied by Ti ions, and then the displacement of the Ti ions from the centre of the octahedra becomes smaller and therefore the electric permittivity and dielectric loss decrease [14].

Moreover, the variation of electric permittivity is also dependent on the polarizability of R ion and it decreases with the decrease in its polarizability [5]. The decrease in the electric permittivity with increase in Sm substitution for La could also be due to the low polarizability of Sm (4.74 Å^3) as compared to La (6.03 Å^3) [15].

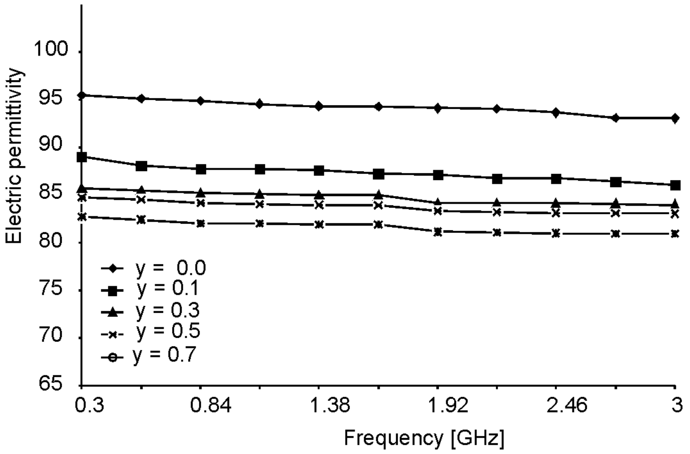

Fig. 5. Variation of electric permittivity with frequency for different Sm contents

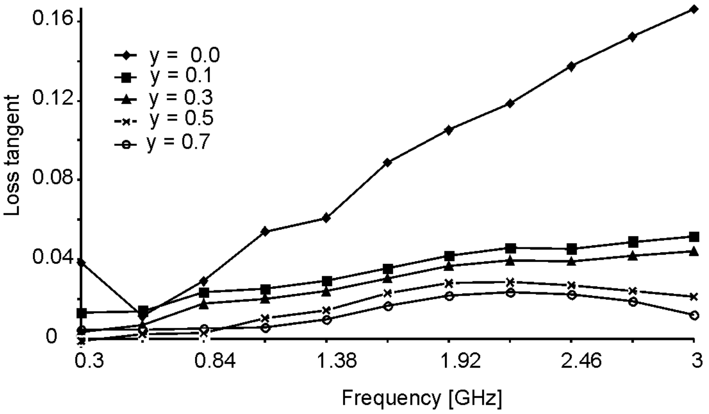

Fig. 6. Variation of loss tangent with frequency for different Sm contents

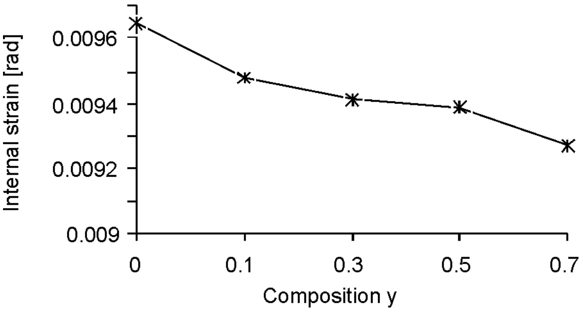

Fig. 7. Dependence of internal strain on Sm contents

Ohsato [5] had shown that the crystal structure with large size difference between Ba and R ions has the excellent quality factor as it has low internal strain. The variation of internal strain in fuction of different Sm contents is shown in Fig 7. With increase in Sm substitution for La, the internal strain decreases and hence the loss tangent also decreases.

4. Conclusions

Microwave dielectric ceramics $Ba_4(La_{(1-y)}Sm_y)_{9.33}Ti_{18}O_{54}$ with $y = 0.0$–0.7 were synthesized using conventional mixed oxide route. These were then characterized for their dielectric and structural properties. The electric permittivities were 93.03–81.02 and loss tangents were 0.1659–0.012 as $y = 0.0$–0.7 at 3.0 GHz. It has been found that substitution of Sm results in reducing the tangent loss with a slight decrease in electric permittivity. The excellent microwave dielectric properties were obtained for $y = 0.5$ with electric permittivity 83.3 and loss tangent 0.021 at room temperature.

Acknowledgements

The authors would like to thank M.L. Sharma (SAIF, Punjab University, Chandigarh, India) for guiding SEM analysis and Gurvinderjit Singh (CAT, Indore, India) helping in analysis of XRD patterns.

References

[1] KOLAR D., STADLER Z., GABERSCEK S., SUVOROV D., Ber. dt. Keram. Ges., 55 (1978), 346.
[2] KOLAR D., GABERSCEK S., VOLAVSEK B., J. Solid. State Chem., 38 (1981), 158.
[3] KAUR D., NARANG S.B., SINGH K., J. Ceram. Proc. Res., 7 (2006), 31.
[4] OHSATO H., OHHASHI T., NISHIGAKI S., OKUDA T., SUMIYA K., SUZUKI S., Jpn. J. Appl. Phys., 32 (1993), 4323.
[5] OHSATO H., J. Eur. Ceram. Soc., 21 (2001), 2703.
[6] OHSATO H., IMAEDA M., Mater. Chem. Phys., 79 (2003), 208.
[7] NARANG S.B., KAUR D., BAHEL S., Mater. Lett., 60 (2006), 3179.
[8] LAFFEZ P., J. Mater. Sci., 30 (1995), 267.
[9] LI Y., CHEN X.M., J. Europ. Ceram. Soc., 22 (2002), 715.
[10] CHENG C.C., HSIEH T.E., LIN I-NAN, Mat. Chem. Phys., 79 (2003), 119.
[11] ANGADI B., JALI V.M., LAGARE M.T., KINI K.S., UMARJI A.M., Bull. Mater. Sci., 25 (2002), 191.
[12] CHEN L.F., ONG C.K., NEO C.P., VARADAN V.V., VARADAN V.K., *Microwave Electronics Measurement and Materials Characterization*, Wiley, New York, 2004.
[13] SHANONON R.D., Acta Cryst., 32A (1976), 751.
[14] OHSATO H., OHHASHI T., KATO H., NISHIGAKI S., OKUDA T., Jpn. J. Appl. Phys., 34 (1995), 187.
[15] SHANNON R.D., J. Appl. Phys., 73 (1993), 348.

Received 3 July 2007
Revised 13 November 2007